Revista Sul-Americana de Engenharia Estrutural
ISSN 2316-2457

ASAEE
Associação Sul-Americana de Engenharia Estrutural

COMPARISON OF RELEVANT PARAMETERS OF THE EXTERNAL FLOW OF A SQUARE CYLINDER BY TWO DIFFERENT TURBULENCE MODELS: RSM AND SST-Kω

Rodolfo A. Carvalho[1*], Lineu J. Pedroso[1]

[1]*Dept. of Civil and Environmental Engineering, University of Brasilia*
SG 12 - Unb, 70297-400, Federal District, Brazil
rodolfoalvescarvalho@yahoo.com.br, lineujp@gmail.com

Abstract. Rectangular cylinders are recurrent in engineering, a particular case is a square. Structures with square shapes are of great interest and their real applications can be seen in columns, towers, counterwind structures of tall buildings, etc. The present work analyses, in bidimensional domain, the external incompressible flow over a cylinder by turbulence models SST-kω and RSM through ANSYS Fluent. In the studied cases the objective is to analyze comparatively relevant parameters of the flow: drag coefficient and Strouhal number. The average pressure coefficient over the cylinder is also evaluated. In all cases analyzed the flow parameters converged to the experimental data. The average pressure coefficient over the cylinder did not present good correlation with the experiments for both turbulence models. The main differences are in the cylinder faces parallel to the flow. The analysis shows that RSM model was able to reproduce accurately the flow parameters. However, this model has a greater computational cost since it adds more equations to be solved and has performed worse than SST-kω model.

Keywords: Square cylinder, RANS Turbulence model, CFD.

1 Introduction

Rectangular cylinders are recurrent in engineering, a particular case is a square. Structures with square shapes are of great interest and their real applications can be seen in columns, towers, counterwind structures of tall buildings, etc.

The flow around square cylinders is poorly studied compared to the circular shape (mainly in function of its symmetry). Considering the practical relevance of the square shape, this study aims to reduce this gap through the numerical modeling of bidimensional, external, turbulent flow around a square cylinder by computational fluid dynamics (CFD) in ANSYS Fluent®. Due to resources limitation, the tridimensional flow was simplified to its equivalent bidimensional.

The scope of this work deals essentially with the numerical bidimensional external flow around a square section representative of a non-aerodynamic prismatic cylinder in monophasic, non-oscillatory and non-uniform flow through CFD. The presented results are preliminary simulations and trials that are in progress at the date of submission of this paper. It is a continuation of previous works of the Dynamics and Fluid-Structure Group of Brasilia University that have been carrying out many studies in CFD in last years in fluid-structure problems, which we quote Pedroso (1998), Ferreira (2012), Santos (2017), Silva (2018), Freitas (2019) and Sarmento et. al (2020).

In this work, through the computational fluid dynamics (CFD), by unsteady RANS (Reynolds Average Navier Stokes) methodology, relevant parameters are evaluated of the

*Corresponding author. rodolfoalvescarvalho@yahoo.com.br
A version of this paper was published in the proceedings of the Ibero-Latin-American Congress on Computational Methods in Engineering ISSN 2675-6269
http://dx.doi.org/10535/rsaee.v19i3.13598

square cylinder studied by Lyn and Rodi (1994). Turbulence effects are resolved by both the turbulent viscosity model SST−kω and the Reynolds Stress Model (RSM). Analyzed parameters are presented by their average value based on 10 (ten) periods of vortex shedding with its standard deviation, commonly missing quantities in similar works.

The drag coefficient (C_d), Strouhal Number (S_t) and the pressure coefficient through the cylinder perimeter are presented, compared, and discussed for both turbulence models.

Although the RSM model studied showed a higher number of equations and consequently higher Computational cost, the SST−kω model, despite its simplicity, performed better face the experimental data.

2 Bibliography Review

Contrary to the circular cylinder, in which the separation point is variable with the Reynolds number, in the rectangular shape it is fixed. According to Berger (1998), due to the corner geometry the separation point occurs in the windward direction for Reynolds number greater than 54.

The turbulent flow around the square cylinder has received less attention than the circular shape. Although similarities can be expected, especially in the wake, differences are constated in length and velocity scales and can present a good correlation between coherent and incoherent (or random) vortex structures.

Bearman [9] shows that bodies with edges have fixed separation points in their corners in which for low Reynolds numbers, when the separation initially occurs, the flow remains stable, although, with the velocity increment, instability occurs yielding transient and random wake behavior.

The firsts researchers' data was obtained from hot-wire anemometer for velocity measurement. In later studies, the experiments were conducted with Laser Doppler velocimetry (LDV) that allows instantaneous velocity measurement, average velocity, and Reynolds stress at a specific point. This technique replaced the hot wire anemometer due to its greater performance and reliability.

Lyn e Rodi (1994) presents field measurements of the velocity field thought LDV technique for a square cylinder in Reynolds number equals 21×10^3. The researchers found a Strouhal (St) of 0.132 ± 0.004.

According to Murakami (1995), the numerical preview of a turbulent flow around a square cylinder is one of the challenging problems in the CFD field. The flow is complicated, characterized by windward sharp corners that induce a steep curvature, recirculation leeward, vortex shedding, among other phenomena.

Numerical studies can be differentiated due to the turbulence model. In the studies, commonly in $Re=22\times10^3$, the domain can be bidimensional or tridimensional. RANS simulations are essentially bidimensional, while LES simulations are seldom though. Direct numerical simulations (DNS) are always tridimensional.

3 Theoretical Foundation

The equations that describe the fluid dynamics have common properties and are described by a general form, known as the transport equation of a general property ϕ. For a general property ϕ (velocity component, pressure, etc) the conservative form (or divergent) for all fluid equations (transport equation) can be written as Eq. (1).

$$\frac{\partial(\rho\phi)}{\partial t} + div(\rho\phi\boldsymbol{u}) = div\big(\Gamma\ grad(\phi)\big) + S_\phi. \tag{1}$$

Each term of eq. (1) represents a transport process that occurs in the flow field, the left-hand side (LHS) terms, local acceleration, and advection, respectively, are equivalent to the right-hand side (RHS) terms, diffusive (Γ is the diffusive constant) and source terms (Sϕ), respectively. The value of ϕ, Γ and Sϕ terms in the equations for mass conservation, momentum, kinetic energy and specific dissipation term (ε) are presented on Tu et al. (2018).

For a stationary control volume in a turbulent flow, the presence of vortex implies net momentum transfer due to convection caused by them. In this way, the flow layers experience additional shear stresses due to turbulence, known as Reynolds stresses. The formulations and constants for the turbulence models studied in this work are presented in ANSYS (2018).

Turbulence Models

The Reynolds averaged equations methodology decomposes the pressure and velocity terms in its average and fluctuation components. This process yields additional terms known as Reynolds's stresses and needs modeling to close the problem.

The widely used models are based on the eddy viscosity (μt) proposed by Boussinesq in 1877. These models assume that Reynold's stresses are proportional to the average deformation rate.

The SST−kω model, presented by Menter [13], combines the advantages of the Wilcox [14] k−ω model, applied in the boundary layer, and the Lauder e Spalding [15] k−ε model, applied in the free flow. The SST−kω model uses a blend function that yields a smooth transition between models.

Reynolds Stresses Models (RSM) applies the general transport equation to solve the Reynolds Stress tensor. In this way, the eddy viscosity hypothesis is not needed since the tensor components are computed by additional transport equations. These models, with higher computational costs, are not widespread and the restricted application. According to Poper [16], RSM models differ in the way they model the specific turbulent kinetic energy dissipation tensor, rate of pressure-deformation tensor, and stress flux tensor.

In this work, two models were studied: The SST−kω model with low Reynolds correction and the RSM model with the quadratic pressure-deformation term, boundary conditions for the wall from turbulent kinetic energy equation and scalable wall function, both are presented in detail in ANSYS (2018).

Numerical Methods

To solve the system of equations, the SIMPLE scheme was utilized for the pressure-velocity couple. This scheme utilizes pressure correctors obtained from the conservation of mass and momentum equations, for the pressure field computation.

The Ansys Fluent obtains the discretized domain and the algebraic system from the finite volume method (FVM). This method discretizes the domain in small control volumes where the transport equations are solved. The general form of the transport equation for an infinitesimal control volume was shown in eq. (1). The fundamental step of this method is the integration of these equations in the small domains, yielding the form of eq. (2).

$$\int_{CV}\left(\frac{\partial(\rho\phi)}{\partial t}\right)dV + \int_{CV} div(\rho\phi\boldsymbol{u})\,dV = \int_{CV} div\big(\Gamma\, grad(\phi)\big)\,dV + \int_{CV} S_{\phi}\,dV. \qquad (2)$$

4 Preliminary Results – Validation and Verification

In this chapter, it will be presented the numerical model, the technique, computational methods utilized, and the boundary conditions. Initially, it is presented a simulation for grid independence test. Then, through relevant flow parameters comparison, the model utilized in this work is validated.

The flow simulated was the same studied by Lyn and Rodi (1994) with Re=22×10^3. The parameters for model validation were obtained from this study.

Computational Model and Boundary Conditions

According to the computational model shown in Fig. 1, the domain size of 27D×20D is the same study by Chen, Djidjeli e Xie [17]. The axis is in the cylinder barycenter and the domain has dimensions 7D windward and 20D leeward. The boundary conditions are inlet prescribed velocity in windward edge, zero gradients in leeward edge, a non-slip condition in the cylinder wall, and symmetry condition in both edges parallel to the flow.

In order to obtain the y+ parameter below 5, the first layer adjacent to the wall height is 3×10^{-5} m. The boundary layer near the wall of the cylinder surface was divided into 200 points to obtain accurate results. The boundary layer was discretized in such a way that it has at least 15 cells in the boundary layer in all situations simulated. In all meshes, the inflation rate from the cylinder wall is 1.03.

The dimensionless time-step in all simulations is $\Delta t^* = \Delta t\, U_0/D = 8.5 \times 10^{-4}$. The Courant number was maintained near 1 ($CFL = u\Delta \mathrm{t}/\mathrm{dx} \approx 1$). To compute the average of flow parameters, after the convergence study, it was utilized a minimum of 10 vortex shedding periods according to Fig. 2.

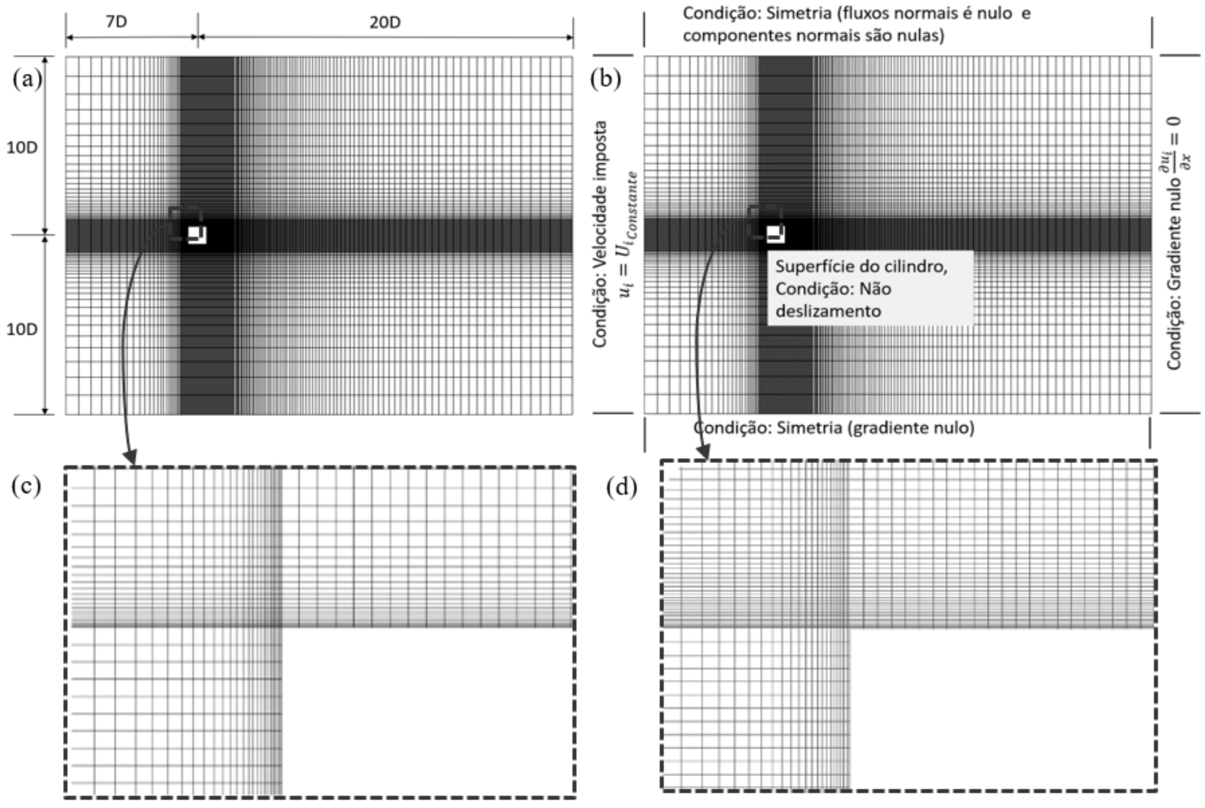

Figure 1 – Computational model, (a) domain, (b) boundary conditions, (c) boundary layer discretization for medium-mesh *and* (d) boundary layer discretization for the fine mesh

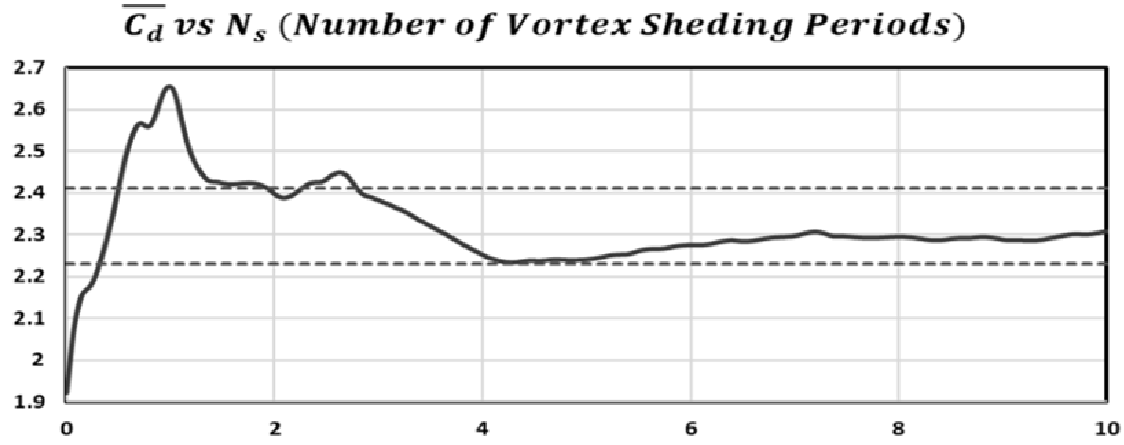

Figure 2 – Number of vortex shedding periods (N_s) for average computation versus average drag coefficient ($\overline{C_d}$)

Grid Independence Teste and Model Validation

For the grid independence test, the RSM model was utilized with quadratic order pressure-deformation. The wall boundary condition was obtained from the turbulent kinetic energy equation. In the wall region, a scalable wall function was utilized.

The SIMPLE scheme for the pressure-velocity was utilized. Despite ANSYS (2018) advice on the utilization of PISO algorithm for transient cases, the test performed shown no increase in performance and higher computational time required in this algorithm. The convergence criteria in each time step were residuals lower than 10^{-6}. The gradient for spatial discretization was computed by the least-squares method based on the cell center. For the pressure term, a second-order scheme was chosen. For the remaining terms, the second-order Upwind scheme was adopted. The implicit second-order scheme was employed in time discretization. A relaxation factor of 0.75 was applied in all variables to optimize the convergence and stability of the solution. The variables extrapolation option was chosen due to its convergence optimization.

For the model validation and grid independence test, according to Tab. 1, relevant flow parameters convergence was analyzed. The parameters were compared with the experimental data presented by Lyn and Rodi (1994).

According to Tab. 1a, the difference between medium and fine mesh was 1.5% for the Strouhal number and 4.6% for the drag coefficient. These values indicate convergence and grid independence. The medium mesh contains 56% fewer cells than the fine mesh, representing a lower computational cost. Thus, it was utilized in the simulations of this work. According to Tab. 1b, for the medium mesh, the differences between the simulations and the experimental data are 6.85% for the Strouhal number and 4.4% for the drag coefficient. These differences indicate a good correlation with the experimental data.

5 Results and discussion

From the numerical model validation and the grid independence test acceptance, the simulations for the RSM and SST−kω models were performed in the validated model.

Tab. 1b shows the results obtained from the simulations for the drag coefficient and the Strouhal number compared to the Lyn and Rodi (1994) experimental data. It can be noticed that the RSM model presented a variation of 4.4% in the drag coefficient and the SST−kω model diverged 3.6% showing greater agreement with the experiments. For the Strouhal number, it can be seen a variation of 6.8% for the RSM model and only 0.8% for the SST−kω.

Table 1 – Comparison of flow relevant parameters: (a) Grid Independence test and (b) numerical simulation results for models RSM e SST-kω

(a)

Author	Medium -Mesh	Fine-Mesh
Nº Cells	47292	84215
C_D	2.19	2.30
Var (%)	-4.6%	0.0%
S_{tr}	0.141	0.139
Var (%)	1.5%	0.0%

(b)

Author	Present, RSM	Present, SST-kω	Lyn and Rodi, 1994
$R_e / 10^4$	2.2	2.2	2.1
S_{tr}	0.141	0.133	0.132
Var (%)	6.8%	0.8%	0.0%
C_D	2.193	2.176	2.100
Var (%)	4.4%	3.6%	0.0%

Fig. 3 shows a comparison of the average pressure coefficient in the ABCD perimeter. Point A is the theoretical stagnation point, point B and C are, respectively, the windward and leeward corners and point D is the center of the rear edge.

In Fig. 3a, for the RSM model, the average pressure coefficient is plotted in red line with its one standard deviation range plotted in traced lines. For comparison, the experimental data presented by Bearman [18] is plotted in a black line. In the stagnation point, the results did not agree with experiments. In the BC region, the experimental data fits inside the one standard deviation region. In the CD region, the reference data is almost inside the considered region.

In Fig. 3b, for the SST-kω model, the average pressure coefficient is plotted in purple line with its one standard deviation range plotted in traced lines. For comparison, the experimental data presented by Bearman [18] is plotted in a black line. In the BC region, the experimental data fits inside the one standard deviation region. In the CD region, the reference data is almost inside the considered region.

In Fig. 3c, both RSM and SST-kω models are compared from their results of average pressure coefficients with Bearman [18] experimental data. In the stagnation point, the results did not agree with the experiment. In BC region, the SST-kω had better agreement with the reference data. In the CD region, a despite good correlation between experimental data and the RSM model, it can be noticed better agreement with the SST-kω model.

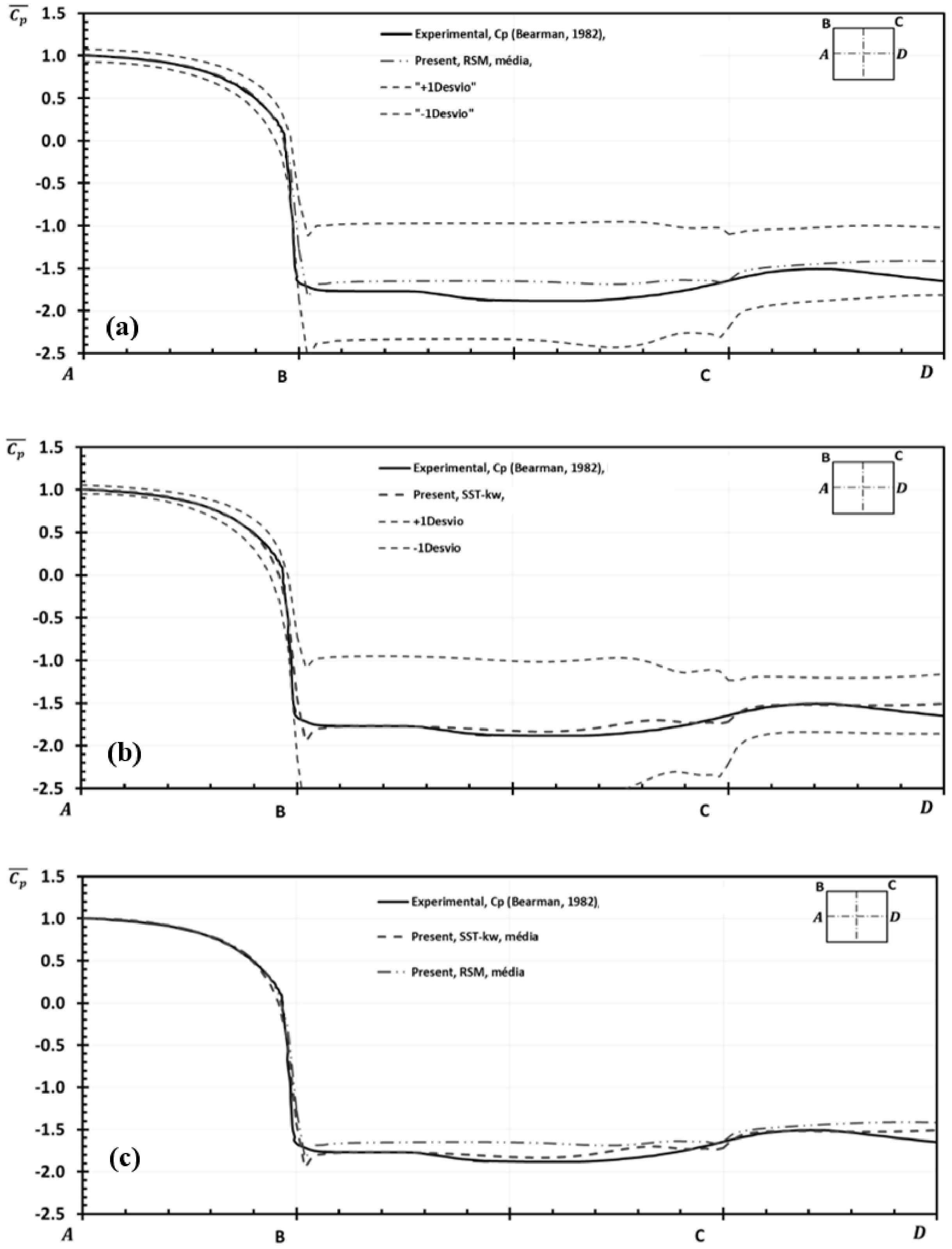

Figure 3. Average pressure coefficient in perimeter ABCD of the cylinder computed from numerical simulations and experiment of Bearman [18]: (a) For RSM with one standard deviation, (b) For $SST - k\omega$ with the one standard deviation range, and (c) for both models: RSM and $SST - k\omega$.

6 Conclusions

Numerical simulation data were compared for the same computational domain with different turbulence models. Although the RSM model has more equations and computational cost, the SST-kω model, despite its simplicity, performed better. In this model, the deviations from the reference values are: (I) for the average drag coefficient it had the shortest deviation (3.6%), and (II) for the Strouhal number it had almost no deviation. The results for the pressure coefficient in the perimeter ABCD were similar for both models and diverges from the experimental data.

The RSM with wall functions was unable to introduce accuracy that justifies its computational cost. Although its lower number of equations, the SST model had the best performance.

References

ANSYS. ANSYS Fluent Theory Guide. ANSYS, Inc, 2018.

Bearman, P. W. Vortex shedding from oscillating bluff bodies. Annual Review of Fluid Mechanics, v. 16, p. 195–222, 1984.

Bearman, P. W.; Obasaju, E. D. An experimental study of pressure fluctuations on fixed and oscillating square-section cylinders. Journal of Fluid Mechanics, v. 119, p. 297–321, jun. 1982.

Berger, E. On A Mechanism Of Vortex Excited Oscillations Of A Cylinder. In: Kramer, C.; Gerhardt, H. J. (Eds.). . Advances in Wind Engineering. Amsterdam: Elsevier, 1988. p. 301–310.

Chen, Y.; Djidjeli, K.; Xie, Z.-T. Large eddy simulation of flow past stationary and oscillating square cylinders. Journal of Fluids and Structures, v. 97, p. 103107, 1 ago. 2020.

Ferreira, J. L. Um Estudo de Ações Dinâmicas em Plataformas Offshore Utilizando Dinâmica dos Fluidos Computacional. Monografia de Graduação, Departamento de Engenharia Civil e Ambiental, Universidade de Brasília, 2012.

Freitas, M.R. CFD Modelling for the Study of Structural Stability of Dams and Spillways Subject to Overtopping. Dissertação de Mestrado, Departamento de Engenharia Civil e Ambiental, Universidade de Brasília, 2019.

L. J. Pedroso, "Interação fluido-estrutura," - *Notas de Curso e Apostila Didática.* UnB-FT/ENC, Brasília, 1998.

Launder, B. E.; Spalding, D. B. Paper 8 - The Numerical Computation Of Turbulent Flows. In: Patankar, S. V. et al. (Eds.). . Numerical Prediction of Flow, Heat Transfer, Turbulence and Combustion. [s.l.] Pergamon, 1983. p. 96–116.

Lyn, D. A.; Rodi, W. The flapping shear layer formed by flow separation from the forward corner of a square cylinder. Journal of fluid Mechanics, v. 267, p. 353–376, 1994.

Menter, F. Zonal Two Equation K-W Turbulence Models For Aerodynamic Flows. In: 23rd Fluid Dynamics, Plasmadynamics, And Lasers Conference. [S.L.] American Institute Of Aeronautics And Astronautics, 2012.

Murakami, S.; Mochida, A. On turbulent vortex shedding flow past 2D square cylinder predicted by CFD. Journal of Wind Engineering and Industrial Aerodynamics, Third Asian-Pacific Symposium on Wind Engineering. v. 54–55, p. 191–211, 1 fev. 1995.

Pope, S. B. Turbulent Flows. Measurement Science and Technology, v. 12, n. 11, p. 2020–2021, out. 2001.

Santos, T. C. Um Estudo de Ações Dinâmicas do Vento em Edifícios Altos. Monografia de Graduação, Departamento de Engenharia Civil e Ambiental, Universidade de Brasília, 2017.

Sarmento, C. V. S.; PEDROSO, L.J. ; RIBEIRO, P. M. V. . From numerical prototypes to real models: a progressive study of aerodynamic parameters of nonconventional concrete structures with Computational Fluid Dynamics. Revista Ibracon de Estruturas e Materiais, v. 13, p. 628-643, 2020.

Silva, A. C. DA. Análise Numérica do Escoamento em Torno de Um Cilindro. Monografia de Graduação. Departamento de Engenharia Civil e Ambiental. Universidade de Brasília, 2018.

Tu, J.; Yeoh, G. H.; Liu, C. Computational fluid dynamics: a practical approach. [s.l.] Butterworth-Heinemann, 2018.

Wilcox, D. C. Reassessment of the scale-determining equation for advanced turbulence models. AIAA Journal, v. 26, n. 11, p. 1299–1310, 1988.